A comparative study of the anisotropy of lattice strain induced in the crystals of L-serine by cooling down to 100 K or by increasing pressure up to 4.4 GPa

Elena V. Boldyreva*[,I,II], Evgenia N. Kolesnik[I,II], Tatyana N. Drebushchak[I,II], Hans Ahsbahs[III], Jon Ares Beukes[IV] and Hans-Peter Weber[IV,V]

[I] Institute of Solid State Chemistry and Mechanochemistry SD RAS, Kutateladze, 18, Novosibirsk, 128, 630128 Russia
[II] REC-008 "MDEST" Novosibirsk State University, Pirogova, 2, Novosibirsk, 90, 630090 Russia
[III] Philipps-Universität Marburg/Lahn, Institute of Mineralogie, Hans-Meerwein Straße, D-35032, Marburg/Lahn, Germany
[IV] European Synchrotron Radiation Facility, Swiss-Norwegian Beamline, P.O. Box 220, F-38043, Grenoble CEDEX, France
[V] Institut de Cristallographie, Universite de Lausanne, CH-1015 Lausanne, Switzerland

Received September 30, 2004; accepted November 6, 2004

L-serine / Lattice strain / Hydrogen bonds / Diamond anvil cell / Low temperatures / Single crystal structure analysis / X-ray diffraction

Abstract. The anisotropy of lattice strain in the crystals of L-serine ($P2_12_12_1$, at ambient conditions $a = 5.615(1)$ Å, $b = 8.589(2)$ Å, $c = 9.346(2)$ Å) on cooling down to 100 K and with increasing hydrostatic pressure up to 4.4 GPa was compared with each other and also with the results previously obtained for the polymorphs of glycine. On cooling, the structure expanded slightly along the crystallographic *a*-direction, compression along the crystallographic *b*- and *c*-directions (normal to the chains of the serine zwitter-ions) was very similar. With increasing pressure, the same structure compressed in all the crystallographic directions, linear strain along *c*-axis was the largest, linear strain along *a*-axis – the smallest, linear compression along the *b*-axis with increasing pressure was slightly larger than that along the *a*-axis. The different anisotropy of lattice strain of the same structure on cooling and under pressure could be correlated with different response of intermolecular hydrogen bonds to these two scalar actions.

Introduction

The variable-temperature and the variable-pressure studies of molecular crystals are helpful for understanding the intermolecular interactions, their role in the formation of a particular structure and in its response to external actions [1–15]. The crystals of amino-acids are of a special interest in this respect, since they can be used as biomimetics, and the data on the response of hydrogen bonds to changes in temperature or pressure in these systems can be used also when considering the properties of biopolymers, in particular – of peptides [11, 13–15]. In our group, we have initiated a systematic comparative study of the anisotropy of lattice strain in the crystals of amino acids and peptides on cooling and with increasing pressure. The results obtained for the simplest amino-acid, glycine, were reported in [14–20]. The next obvious step was to study serine, in which a side $-CH_2OH$-group was added, that can be involved in the extra hydrogen bond formation [16]. The results of this study were preliminary reported at the XLII International Scientific Conference "Students and the Progress in Science and Technology" (Novosibirsk, Russia) [21] and at the 3-rd International Meeting on Phase Transitions at High Pressures (Chernogolovka, Russia) [22]. A detailed description of these results is the subject of the present publication.

Experimental

The effect of cooling on L-serine was studied using a single-crystal X-ray diffraction technique (MoK_α, $\lambda = 0.71069$ Å). Needle-shaped crystals of the anhydrous L-serine were obtained by a rather quick crystallization of the saturated solution of a powder sample of L-serine purchased from ICN Biomedicals in the 1 : 1 ethanol : water mixture [16]. Data collection was done with a STADI-4 four-circle diffractometer (Stoe, Darmstadt). The temperature was controlled with a 600 Series Cryostream Cooler (Oxford Cryosystem) with a gas temperature stability of 0.1 K. Data collection was done at 100, 200, 295 K, and the structure was refined at these temperatures. Crystal data and data collection parameters are summarized in Table 1. Cell parameters were measured in 20–25 K steps in temperature. 30 reflections in the 2θ range between 25 and 30° were used for cell refinement. To increase the precision, each reflection was measured at both sides of the primary beam. An ω-scan was carried out at + and -2θ and ω, the centre of gravity was determined for both scans, and the observed 2θ was given by the difference of the two ω centres, eliminating zero point errors.

* Correspondence author (e-mail: boldyrev@nsu.ru)

Table 1. Crystal data, data collection, and structure refinement summary.

Formula	$C_3H_7NO_3$
Molecular weight	105.12
Crystal size (mm)	$0.12 \times 0.19 \times 0.69$
Crystal system	Orthorhombic
Space group	$P2_12_12_1$, $Z = 4$
Radiation (Å)	MoK_α ($\lambda = 0.71069$)
Monochromator	Graphite
Detector	Scintillation counter
Data collection	$2\theta/\omega$ scans
Structure solution	Direct methods, SHELXS [23, 24]
Structure refinement	SHELXL [25]. All non-hydrogen atoms anisotropic, H-atoms isotropic from the Fourier difference maps. Refined on F^2.

Temperature, K	100	200	295
D_{calc} (g cm^{-3})	1.574	1.562	1.549
N_{meas}	4608	3508	3920
N_{indep}	1958	1682	1993
$N_I > 2\sigma$ (I)	1783	1394	1464
R_{int}	0.0393	0.0358	0.0314
θ_{max}	35.05	35.05	35.04
h	$-9 \rightarrow 9$	$-7 \rightarrow 9$	$-9 \rightarrow 9$
k	$-13 \rightarrow 13$	$-13 \rightarrow 12$	$-13 \rightarrow 13$
l	$-14 \rightarrow 14$	$-15 \rightarrow 13$	$-15 \rightarrow 15$
$R_1(F^2 > 2\sigma(F^2))$	0.0323	0.0496	0.0503
$R_1(F^2)$, all	0.0392	0.0687	0.0828
$wR(F^2)$	0.0786	0.1154	0.1067
N parameters	92	92	92
S	1.079	1.094	1.100
$\Delta\varrho_{max}$ (e Å^{-3})	0.287	0.275	0.285
$\Delta\varrho_{min}$ (e Å^{-3})	−0.214	−0.227	−0.220

The effect of pressure on the structure of L-serine was followed using an X-ray powder diffraction technique using a monochromatized synchrotron radiation source at the Swiss-Norwegian Beam Line at ESRF ($\lambda =$ 0.71950 Å, collimator width and height 0.15 mm). Diffraction patterns were registered with a MAR345 image plate detector (pixel size 0.15 mm, 2300×2300 pixels in image, maximum resolution 1.105 Å, maximum 2θ 36.942°). The frames were measured with exposing time equal to 900–3600 seconds, with oscillation in $\varphi \pm 3$ degrees. The distance from crystal to detector, the beam center position, the tilt angle and the tilt plane rotation angle were refined using a Si standard put at a diamond anvil of the open DAC in a special calibration experiment. Hydrostatic pressure was created in a DAC of the four-screw type (Merrill-Bassett type cell modified by Mao & Bell [26–28]). "Thyrodur 1.2709" – steel was used as a gasket material. After the gasket was preliminary pressed to the thickness of 0.077 mm, it was hardened by heating at 500 °C with subsequent cooling [29]. A dry methanol-ethanol mixture was used as a pressure-transmitting medium [30]. The sample in the DAC was centered with respect to the beam very carefully, so that no reflections from steel gasket could be observed in the measured diffraction pattern. Ruby fluorescence was used for pressure calibration [31, 32]. Fit2D program [33] was used for processing diffraction data measured with the synchrotron source (calibration, masking, integration). A Program Collection POLYCRYSTAL [34] was used to refine the cell parameters from the measured values of theta-angles and the *hkl*-indices ascribed to the diffraction lines on the basis of the ambient-pressure structure of L-serine [35, 36] and the analysis of the changes in the d_{hkl}-values in the diffraction patterns versus pressure. The pressure range up to 4.4 GPa was selected, in which no phase transitions in L-serine were observed. PowderCell [37] and Platon [38] were used for structure analysis and graphic representation. No special program was needed to calculate strain tensors, since the structure of L-serine is orthorhombic [35, 36] and the strain tensor axes coincide with the crystallographic axes [39].

Results and discussion

The changes in cell parameters and cell volume of L-serine as a function of temperature and pressure are summarized in Table 2 and in Table 3, correspondingly. No phase transitions took place in this temperature and pressure range. The structure preserved the space group symmetry $P2_12_12_1$ (at ambient conditions $a = 5.615(1)$ Å, $b = 8.589(2)$ Å, $c = 9.346(2)$ Å). The data on the atomic coordinates and anisotropic displacement parameters at temperatures 100, 200, 295 K were deposited as CIFs at Cambridge Crystallographic Data Centre, Nos. CCDC 249277, CCDC 249278, CCDC 249279[1].

Table 2. Cell parameters and cell volume of L-serine at several temperatures (* from reference [35]; ** from reference [36]).

T (K)	a (Å)	b (Å)	c (Å)	V (Å^3)
325	5.6130(11)	8.6051(22)	9.3583(25)	452.01(15)
300	5.6145(12)	8.591(3)	9.347(3)	450.84(17)
295	5.6140(9)	8.5886(18)	9.3447(20)	450.56(12)
295	5.6149(9)	8.5889(19)	9.3457(21)	450.70(13)
295*	5.618(2)	8.599(5)	9.348(3)	456.58(3)
295**	5.615(2)	8.571(2)	9.325(3)	448.78(2)
275	5.6158(9)	8.578(19)	9.3371(21)	449.82(13)
250	5.6171(11)	8.5665(23)	9.325(10)	448.72(15)
225	5.6189(15)	8.556(3)	9.316(3)	447.87(20)
200	5.6193(17)	8.545(3)	9.305(5)	446.7(3)
200	5.6193(17)	8.545(3)	9.305(4)	446.78(23)
200	5.6193(17)	8.546(4)	9.305(4)	446.84(23)
175	5.6201(17)	8.536(3)	9.295(4)	445.89(23)
150	5.6204(19)	8.529(4)	9.285(4)	445.1(3)
125	5.6201(15)	8.524(3)	9.274(3)	444.30(19)
100	5.6193(14)	8.519(3)	9.265(3)	443.51(19)

[1] These data can be obtained free of charge via www.ccdc.cam.ac.uk/data_request/cif, by emailing data_request@ccdc.cam.ac.uk, or by contacting The Cambridge Crystallographic Data Centre, 12, Union Road, Cambridge CB2 1EZ, UK; fax: +44 1223 336033.

Table 3. Cell parameters and cell volume of L-serine at several pressures.

P (GPa)	a (Å)	b (Å)	c (Å)	V (Å^3)
0.0001	5.6140(9)	8.5886(18)	9.3447(20)	450.56(24)
0.3	5.5948(15)	8.534(4)	9.235(5)	440.9(6)
0.6	5.5965(23)	8.516(6)	9.214(7)	439.1(7)
1.0	5.5728(16)	8.463(5)	9.097(5)	429.0(6)
1.5	5.5590(17)	8.437(5)	9.003(5)	422.2(6)
1.9	5.5445(10)	8.416(3)	8.918(3)	416.15(36)
2.35	5.5324(14)	8.404(4)	8.864(4)	412.1(5)
2.8	5.5146(14)	8.379 (3)	8.813(5)	407.3(5)
3.25	5.5076(21)	8.349(5)	8.741(8)	401.9(7)
3.65	5.4918(24)	8.331(6)	8.708(9)	398.4(9)
3.95	5.4827(27)	8.317(6)	8.670(10)	395.4(9)
4.4	5.4741(26)	8.296(6)	8.634(9)	392.1(9)
4.0	5.4802(22)	8.317(5)	8.668(8)	395.1(8)
3.2	5.5064(20)	8.346(4)	8.756(7)	402.4(7)
2.4	5.5349(16)	8.401(4)	8.862(5)	412.1(5)
1.7	5.5530(18)	8.425(5)	8.952(5)	418.8(6)
1.2	5.5730(19)	8.455(4)	9.057(6)	426.8(6)
0.94	5.5774(19)	8.478(5)	9.097(6)	430.1(6)
0.3	5.5940(21)	8.511(6)	9.202(7)	438.1(8)

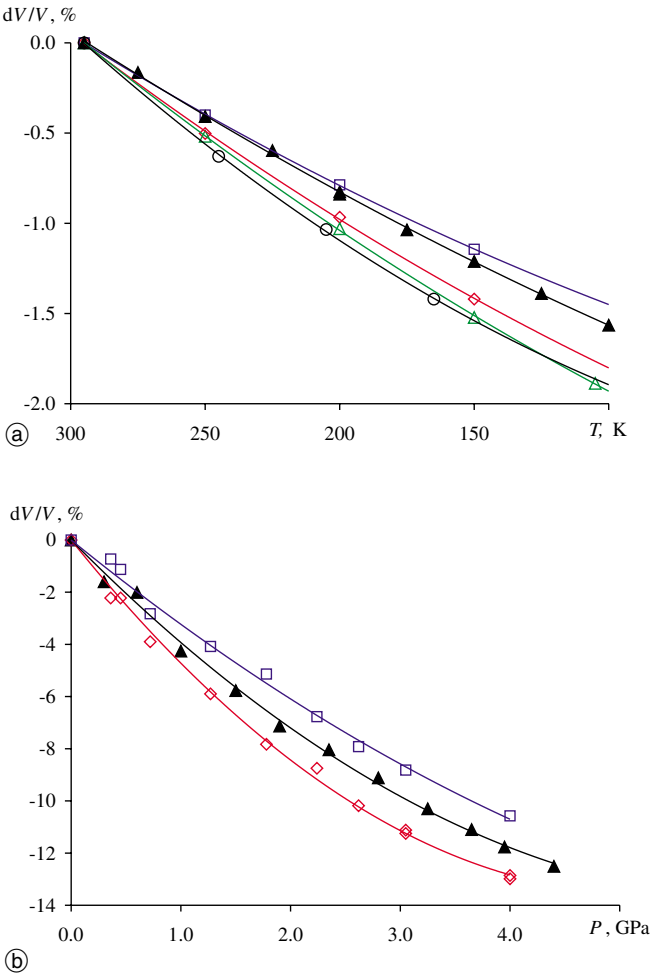

Fig. 1. Relative volume changes on cooling (**a**) and with increasing pressure (**b**) for L-serine (black triangles); for a comparison, data for the polymorphs of glycine (red rhombs – α-form, green triangles – β-form, blue squares – γ-form) [17, 18] and L-alanine (white circles) [40] are also plotted. (The figure is in color in the electronic version only.)

Relative bulk compression on cooling in L-serine was comparable with that previously measured for γ-glycine (being slightly larger), and noticeably smaller, than the values measured for the α- and the β-polymorphs of glycine [18], or L-alanine [40] (Fig. 1a). For example, relative volume changes on cooling down from ambient temperature to 100 K were −1.6% for L-serine, −1.4% for γ-glycine, −1.8% for α-glycine, −1.9% for β-glycine and −1.9% for L-alanine. Relative bulk compression of L-serine with increasing pressure had a value between those measured for the γ- and the α-polymorphs of glycine [17] (Fig. 1b). For example, an increase in pressure from ambient up to 4 GPa resulted in a relative volume decrease equal to −11.8% for L-serine, −12.9% for α-glycine, −10.6% for γ-glycine.

To change the volume of L-serine at −1.6%, would require either to cool the sample down to 100 K, or to increase pressure up to 0.4 GPa. Still, this change in volume would be achieved by a qualitatively different anisotropic structural distortion. On cooling, the structure compressed along the crystallographic directions of the two

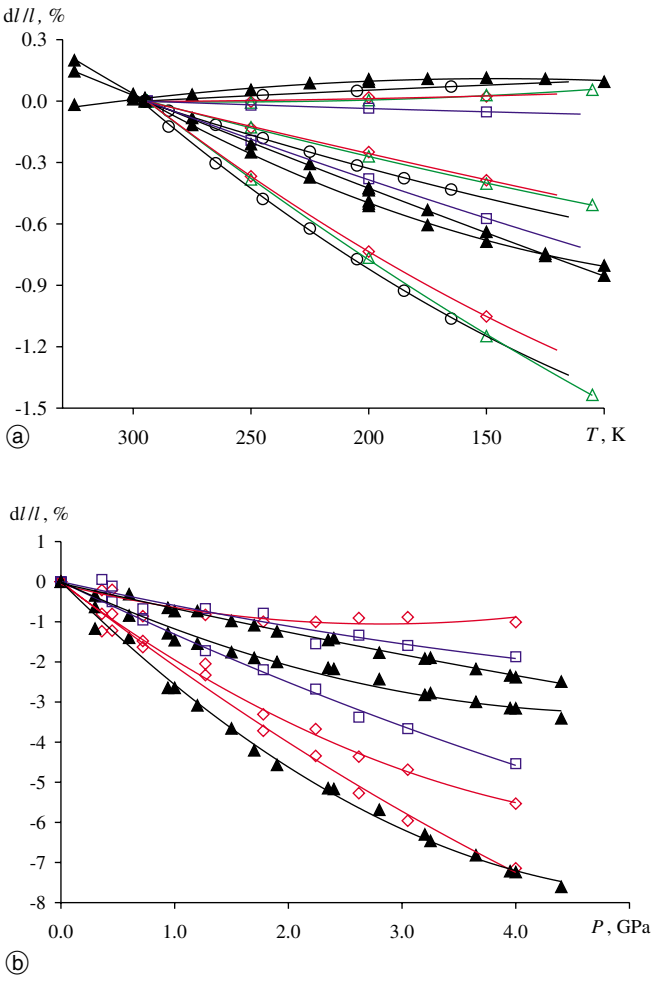

Fig. 2. Relative linear strain along the principal axes (1, 2, 3) of strain ellipsoids on cooling (**a**) and with increasing pressure (**b**) for L-serine (black triangles); for a comparison, data for the polymorphs of glycine (red rhombs – α-form, green triangles – β-form, blue squares – γ-form) [17, 18] and L-alanine (white circles) [40] are also plotted. Axis 1 – minimum linear size of strain ellipsoid, axis 3 – maximum linear size of strain ellipsoid, axis 2 is normal to 1 and 3. (The figure is in color in the electronic version only.)

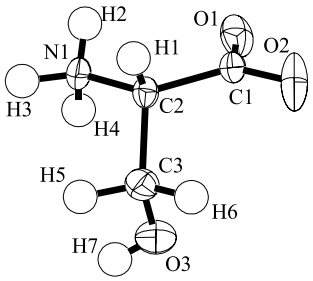

Fig. 3. A molecule of L-serine at 295 K. Atomic displacement parameters correspond to 50% probability. Hydrogen atoms were refined isotropically.

longer cell axes, b and c (the compressibility in the $(b \times c)$ plane being almost isotropic), and expanded slightly along the shortest a-axis (Fig. 2a). The anisotropy of strain induced by increasing pressure was different from that on cooling: the structure compressed in all the crystallographic directions, compression along axis a being slightly smaller than that along b, and about three times smaller than that along c (Fig. 2b).

The structural expansion of L-serine along a on cooling (0.1% on cooling from 300 K down to 100 K) was very similar to the one measured previously for L-alanine (0.07% on cooling from 300 K down to 165 K) [40], α- and β-glycine (0.02% and 0.03% on cooling from 300 K down to 150 K) [18]. The maximum linear compression in L-serine on cooling was comparable with that in γ-glycine [18], and about 1.6 times smaller than the maximum linear compression in L-alanine [40], α- and β-glycine [18] (Fig. 2a). Maximum linear strain in the structure of L-serine with increasing pressure was comparable with the corresponding value previously measured for α-glycine and larger than that in γ-glycine [17]. Minimum linear strain in the structure of L-serine with increasing pressure was comparable with the corresponding value reported for γ-glycine [17] (Fig. 2b).

The crystal structure of L-serine is formed by zwitter-ions (Fig. 3) linked via NH . . . O hydrogen bonds into "head-to-tail" chains along the crystallographic axis a. Every NH_3-group in the chain forms two NH . . . O hydrogen bonds with the neighbouring carboxyl group: a short bond with one oxygen atom (bond 1) and a long bond with another oxygen atom (bond 2). The chains of zwitter-ions of L-serine are linked via extra NH . . . O hydrogen bonds into a 3D-network. In the plane $(a \times b)$, the neighbouring chains are antiparallel to each other and are linked by the hydrogen bonds NH . . . O along b (bond 3). In the plane $(a \times c)$, the neighbouring chains of the zwitter-ions are parallel to each other and are related by a 2_1 screw axis parallel to axis a. Every chain is linked to one neighbouring chain in the plane via NH . . . O hydrogen bonds (bond 4 along c axis) and with another neighbouring chain via OH . . . O bonds between the side CH_2OH groups (bond 5 along axis a) (Fig. 4).

The directions of the principal axes of strain ellipsoids on cooling and with increasing pressure coincide with the a, b, and c crystallographic directions in the structure of L-serine and can be correlated with the structure of the NH . . . O and OH . . . O hydrogen bond network (Fig. 4).

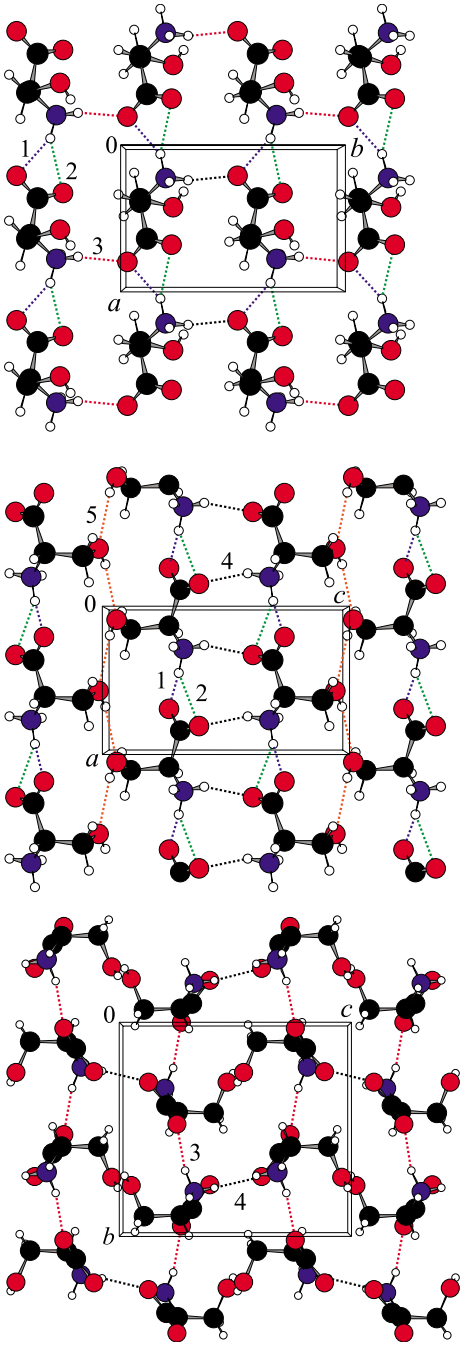

Fig. 4. Fragments of the crystal structure of L-serine explaining the numeration of H-bonds used in this paper. Black circles – C, small white circles – H, dashed circles (in color version – blue) – N, large white circles (in color version – red) – O.

The most rigid (both on cooling and with increasing pressure) direction in the structure of L-serine is the direction along axis a, corresponding to the shortest cell parameter. It coincides with the direction of the "head-to-tail" chains formed by serine-zwitter-ions (Fig. 4). Similar chains are present in many other amino-acid crystal structures [19, 20, 40–44], and can be supposed to be the "structure-forming synthones" in these systems. For example, they were shown to be preserved in all the polymorphs of glycine, including the recently described high-pressure δ-form [19, 20, 42–44]. The structures of all the polymorphs of glycine, and of L-alanine were reported to have the minimum linear strain in the directions of these

chains on cooling (the structures of α-glycine, β-glycine, L-alanine expand slightly in these directions with decreasing temperature) [18, 40]. For the α-, γ-, and δ-glycine the directions of these chains were shown to be the most rigid also when applying pressure to the samples [17, 19]. With increasing pressure, the structure of α-glycine first compresses slightly and then starts to expand in the direction of the "head-to-tail" chains [17]. The structure of L-serine expands along these chains on cooling and compresses with increasing pressure. The compression of the structure of L-serine along axis *b* on cooling is comparable with that along axis *c*. In contrast to that, with increasing pressure the same structure compressed noticeably less along *b* direction, than along *c* axis (Fig. 2).

The different anisotropy of lattice strain of the same structure of L-serine on cooling and under pressure is remarkable. Earlier, the striking differences in anisotropy of structural strain on cooling and with increasing pressure were reported for Co(III) nitroammine complexes [45–47], and the polymorphs of paracetamol [48–51]. The anisotropy of strain on cooling and with increasing pressure is not the same also for sodium oxalate [52], or for the α- polymorph of glycine [14, 17, 18]. In the α-glycine the most rigid (and even slightly expanding) direction in the structure is the same for the strain induced by cooling and by increasing pressure (along the "head-to tail" chains). At the same time, with increasing pressure, the largest compression of the structure was observed in the plane of the layers formed by glycine zwitter-ions, in the direction of the bonds linking the "head-to tail" chains with each other to form a layer. On cooling, the same structure was most compressible in the direction normal to these planes. The difference between the compressibility within a molecular layer and in the direction normal to it was rather small with increasing pressure, but quite pronounced – on cooling (Fig. 2) [17, 18]. For the γ-glycine, however, the anisotropy of strain on cooling and with increasing pressure was similar [17, 18]. Very similar structural distortion on cooling and with increasing pressure, also through the phase transition point, was reported for 1,3-cyclohexanedione [53, 54].

The different response of the same structure to cooling and to increasing pressure may be related to different relative compressibility of the different types of hydrogen bonds in the same structure. For example, on cooling, both in the monoclinic and in the orthorhombic polymorphs of paracetamol the longer NH...O bonds shorten more, than the shorter (and, presumably, stronger) OH...O bonds [51]. The result is essentially different from the effect observed in the monoclinic form with increasing pressure, when the NH...O bonds are less compressible than the OH...O bonds [48].

It is also important to compare the changes in the intramolecular geometric parameters (bond lengths, bond angles, torsion angles).

The values of selected intramolecular geometric parameters for L-serine at variable temperatures are summarized in Table 4. The C−C and C−N intramolecular bond lengths in L-serine are very similar with the values reported for the polymorphs of glycine [18]. The two CO-bonds of the carboxyl group in L-serine are shorter, and differ in length more, than the corresponding two bonds in glycine. On cooling, these two bonds in L-serine expand quite noticeably (at about 0.01 Å at 100 K). In the polymorphs of glycine the two CO-bonds also showed the tendency to expand on cooling, but this elongation was almost within the error limit (about 0.005 Å at 100 K) [18]. A similar effect was observed in the polymorphs of paracetamol – on cooling [51] and with increasing pressure [48–50]. The lengthening of the C=O bond on compression of the O...HO hydrogen contacts was observed also for a series of molecular crystals [1]. The values of the bond angles OCC, OCC, CCN are practically the same in L-serine and in glycine, whereas the values of some of the torsion angles differ very much. For example, the difference in the value of the OCCN angle is about 20°. On cooling, the value of this torsion angle also changes measurably – at about 1.5°.

The changes in the geometric parameters characterizing various types of hydrogen bonds and the distortion of the chains of serine zwitter-ions along *a*-axis in the structure of L-serine on cooling are summarized in Table 5. At ambient temperature, the shorter NH...O hydrogen bond (1) linking serine zwitter-ions in a "head-to-tail" chain is noticeably longer than the corresponding NH...O bonds in α-, β-, γ-glycine [18], or L-alanine [40]. At the same time, it is also much more compressible on cooling, than the corresponding hydrogen bonds in the crystals of glycine polymorphs (ten times more compressible than the bond in α-glycine) [18]. The longer NH...O bond in the same chain (bond 2), on the contrary, is noticeably shorter in L-serine, than are the corresponding "bonds" in the polymorphs of glycine, or in L-alanine [40] (where the distance N...O is actually larger than is necessary to qualify the NH...O contact as a hydrogen bond). On cool-

Table 4. Selected intramolecular bond lengths (Å) and angles (°) in L-serine (labeling of atoms is explained in Fig. 3).

Geometric parameter	100 K	200 K	295 K
O1−C1	1.2502(11)	1.2443(19)	1.2388(19)
O2−C1	1.2617(11)	1.2590(19)	1.2509(19)
C2−C1	1.5319(12)	1.532(2)	1.533(2)
C2−C3	1.5244(12)	1.519(2)	1.514(2)
N1−C2	1.4852(11)	1.4821(19)	1.4829(19)
O3−C3	1.4311(12)	1.430(2)	1.428(2)
N1−C2−C3	109.95(7)	110.15(13)	110.22(13)
N1−C2−C1	110.86(7)	110.78(11)	110.71(11)
C3−C2−C1	111.51(7)	111.79(12)	112.12(12)
O3−C3−C2	110.30(7)	110.03(13)	109.96(13)
O1−C1−O2	125.50(8)	125.44(14)	125.48(14)
O1−C1−C2	118.16(7)	118.20(13)	118.24(12)
O2−C1−C2	116.34(7)	116.35(13)	116.27(13)
N1−C2−C3−O3	60.99(9)	61.05(17)	61.04(17)
C1−C2−C3−O3	−62.39(9)	−62.56(17)	−62.78(18)
N1−C2−C1−O1	−0.15(10)	0.24(19)	0.2(2)
C3−C2−C1−O1	122.71(8)	123.50(15)	123.73(16)
N1−C2−C1−O2	−179.59(7)	−178.99(14)	−178.72(14)
C3−C2−C1−O2	−56.73(10)	−55.73(19)	−55.18(19)

Table 5. Interatomic distances (Å) and angles (°) in the hydrogen bonds in the structure of L-serine.

T (K)	D	H	A	D−H	H−A	D(H)−A	D−H−A
1. O at $(-1 + x, y, z)$ (the shorter H-bond in the head-to-tail chains)							
100	N1	H3	O2	0.961(18)	1.927(17)	2.8296(11)	155.5(14)
200	N1	H3	O2	0.94(3)	1.96(3)	2.8468(19)	157(2)
295	N1	H3	O2	0.97(3)	1.97(3)	2.8700(19)	152(2)
2. O at $(-1 + x, y, z)$ (the longer H-bond in the head-to-tail chains)							
100	N1	H3	O1	0.961(18)	2.340(18)	3.1294(12)	139.0(12)
200	N1	H3	O1	0.94(3)	2.36(3)	3.126(2)	138(2)
295	N1	H3	O1	0.97(3)	2.29(3)	3.1116(18)	141(2)
3. O at $(1 - x, 0.5 + y, 1.5 - z)$ (the H-bond between antiparralel chains within a layer)							
100	N1	H4	O2	0.942(13)	1.939(13)	2.8616(13)	166.1(13)
200	N1	H4	O2	0.92(2)	1.98(2)	2.869(2)	162.7(19)
295	N1	H4	O2	0.941(19)	1.962(19)	2.874(2)	162.7(19)
4. O at $(-0.5 + x, 0.5 - y, 2 - z)$ (the H-bond between the ab-layers)							
100	N1	H2	O1	0.926(16)	1.936(16)	2.8202(14)	158.9(16)
200	N1	H2	O1	0.87(3)	2.01(3)	2.829(2)	156(3)
295	N1	H2	O1	0.88(3)	2.01(3)	2.841(2)	158(3)
5. O at $(-0.5 + x, 0.5 - y, 1 - z)$ (along the head-to-tail chains)							
100	O3	H7	O3	0.81(2)	2.17(2)	2.9068(8)	150.8(18)
200	O3	H7	O3	0.75(4)	2.24(4)	2.9134(11)	150(3)
295	O3	H7	O3	0.78(4)	2.24(3)	2.9181(8)	146(3)

ing, this long bond expands in the structure of L-serine, whereas it compresses in the structures of glycine polymorphs.

In the structure of L-serine all the intermolecular hydrogen bonds linking zwitter-ions in a chain shortened on cooling, and the expansion of the chain was due to the angular distortions, in particular due to an increase (at about 5° at 100 K) in the value of the O−H−O angle in the O−H...O hydrogen bonds involving the side CH_2OH-groups of the serine zwitter-ions, and the changes of torsion angles in L-serine zwitter-ions (Tables 4, 5). It is not the first example of a negative thermal expansion of a structure in a particular direction due to angular distortions. The structure of the monoclinic polymorph of paracetamol, for example, was shown to expand with increasing pressure along the direction of the NH...O hydrogen bonds despite the shortening of these bonds due to the flattening of the molecules and their rotation with respect to each other [48]. The expansion of the structure of the orthorhombic paracetamol on cooling in the direction of the crystallographic a axis could not be explained without taking into account the changes in the torsion angles of the paracetamol molecules, since all the intermolecular hydrogen bonds in the structure shorten, also the OH...O bonds linking the molecules in the chains close to the a-direction [51]. Shortening of intermolecular hydrogen bonds was shown to be related to conformational changes in pentaerithriol [55].

The interchain hydrogen bonds NH...O in the structure of L-serine (bonds 4 along axis c) are shorter at all the temperatures than the interchain NH...O bonds in the α- and β-glycine, but longer, than such bonds in the γ-glycine. The compressibility of these type of bonds is similar in the polymorphs of glycine and in L-serine (the same for L-serine and γ-glycine, slightly smaller for α- and β-glycine). The other interchain NH...O bonds in L-serine (bonds 3 along axis b) are longer than NH...O hydrogen bonds in the polymorphs of glycine, and are also somewhat less compressible on cooling. The compressibility of bonds 4 on cooling is about 1.7 times higher than the corresponding value measured for bonds 3 (Table 5). At the same time, the linear strain of the crystal structure on cooling is almost the same in the directions of the axes b and c (Fig. 2, 4c). This illustrates once again that there is not always a direct correlation between linear strain in a particular direction in the crystal structure and the changes in the interatomic distances in a hydrogen bond in the same direction; conformational changes in the molecules and rotations of the molecules must be also taken into account. It is interesting to note, that when the same structure is subjected to high pressure, the linear strain along b and c axes is no longer the same (Fig. 2). A similar (but, in some sense, a reverse) effect was observed for the orthorhombic polymorph of paracetamol: despite a different compressibility of the NH...O and OH...O bonds with increasing pressure, the structure compressed isotropically in the crystallographic plane comprising the molecules linked via these hydrogen bonds [49], whereas this did not hold for the strain induced by cooling [51].

Conclusions

The study has shown that the structural strain induced in the crystals of L-serine is similar in some respects to that previously measured for the three polymorphs of glycine.

The "head-to-tail" chains formed by zwitter-ions are present in all the crystal structures and behave rather similarly on cooling and with increasing pressure. All the structures were shown to be the most rigid in these directions. The presence of the polar side $-CH_2OH$ groups forming extra OH...O hydrogen bonds as compared to the polymorphs of glycine did not change much the response of the structure to the changes in temperature or pressure. Maybe this is because the direction of these extra OH...O bonds in the structure of L-serine coincides with the direction of the rigid "head-to-tail" chains of zwitter-ions, and the properties of the structure are determined mainly by the properties of these chains.

A detailed comparative analysis of the structural changes induced in the crystals of L-serine on cooling and with increasing pressure has also revealed pronounced differences in the effect of the same scalar action on the same structure. Similar effect was observed earlier for several compounds. Its nature requires further studies and can be related, in particular, to different response of hydrogen bonds to changes in temperature and in pressure. When discussing the anisotropy of structural strain, in addition to comparing the compressibility of various NH...O and OH...O hydrogen bonds, it is essential to take into consideration the conformational transformations of molecular geometry.

Acknowledgments. The study was supported by a grant from BRHE (NO-008-X1), a grant from RFBR (02-03-33358), grants UR.05.01.21, 3H-67-01 and 0069 ("Integration") from Russian Ministry of Education, and a grant from the Russian Science Support Foundation (EB).

References

[1] Katrusiak, A.: High-pressure X-ray diffraction studies on organic crystals. Cryst. Res. Technol. **26** (1991) 523–531.
[2] Katrusiak, A.: Geometric effects of H-atom disordering in hydrogen-bonded ferroelectrics. Phys. Rev. **B48** (1993) 2992-3002.
[3] Katrusiak, A.: Coupling of displacive and order-disorder transformations in hydrogen-bonded ferroelectrics. Phys. Rev. **B51** (1995) 589–592.
[4] Katrusiak, A.: Macroscopic and structural effects of hydrogen-bond transformations. Crystallogr. Rev. **5** (1996) 133–180.
[5] Boldyreva, E. V.: Interplay between intra- and intermolecular interactions in solid-state reactions: general overview, in: Reactivity of Molecular Solids (1999). (E. Boldyreva and V. Boldyrev, Eds), Wiley: Chichester, 1–50.
[6] Hemley, R. J.; Dera, P.: Molecular crystals. Rev. Mineral. Geochem. **41**, High-Temperature and High-Pressure Crystal Chemistry. Mineral. Soc. America (2000) 335–419.
[7] Katrusiak, A.: Pressure-induced H-transfers in the networks or hydrogen bonds. In: Frontiers of High-Pressure Research (Eds. H. D. Hochheimer, B. Kuchta, P. K. Dorhout, J. L. Yager), p. 73–85. Kluwer Academic Publishers, Dordrecht/Boston/London 2001.
[8] Katrusiak, A.: Macroscopic and structural effects of hydrogen-bond transformations. Crystallography Reviews **9** (2003) 91–133.
[9] Boldyreva, E. V.: High-pressure studies of the anisotropy of structural distortion of molecular crystals. J. Molec. Struct. **647** (2003) 159–179.
[10] High-Pressure Crystallography, NATO Science Series, II. Mathematics, Physics, Chemistry (Eds A. Katrusiak, P. McMillan), Vol. **140** Kluwer, Dordrecht 2004.
[11] Boldyreva, E. V.: Molecules in strained environment. In: High-Pressure Crystallography. NATO Science Series, II. Mathematics, Physics, Chemistry (Eds A. Katrusiak, P. McMillan), p. 495–512. **Vol. 140** Kluwer, Dordrecht 2004.
[12] Katrusiak, A.: General description of hydrogen-bonded solids at varied pressures and temperatures, *In: High-Pressure Crystallography.* A. Katrusiak & P. McMillan (Eds), NATO Science Series, II. Mathematics, Physics, Chemistry, Vol. 140, 2004, Kluwer: Dordrecht, 513–520.
[13] Boldyreva, E. V.: High-pressure studies of the hydrogen bond networks in molecular crystals. J. Molec. Struct. **700** (2004) 151–155.
[14] Boldyreva, E. V.: High-pressure induced structural changes in molecular crystals preserving the space group symmetry: anisotropic distortion/isosymmetric polymorphism. Cryst. Engineering **6/4** (2004) 235–254.
[15] Boldyreva, E. V.: High pressure and supramolecular systems. Russian Chem. Bulletin **53** (2004) 1315–1324.
[16] Kolesnik, E. N.: Variable-temperature/variable-pressure study of the crystal structures of amino acids and dipeptides. Master Thesis, Novosibirsk State University (2004) 47 pp.
[17] Boldyreva, E. V.; Ahsbahs, H.; Weber, H.-P.: A comparative study of pressure-induced lattice strain of α- and γ-polymorphs of glycine. Z. Kristallogr. **218** (2003) 231–236.
[18] Boldyreva, E. V., Drebushchak, T. N.; Shutova, E. S.: Structural distortion of the α-, β-, and γ-polymorphs on cooling. Z. Kristallogr. **218** (2003) 366–376.
[19] Boldyreva, E. V.; Ivashevskaya, S. N.; Sowa, H.; Ahsbahs, H.; Weber, H.-P.: Effect of high pressure on the crystalline glycine: a new high-pressure polymorph formation. Doklady Chem. **396** (2004) 358–361.
[20] Boldyreva, E. V.; Ivashevskaya, S. N.; Sowa, H.; Ahsbahs, H.; Weber, H.-P.: Effect of hydrostatic pressure on the γ-polymorph of glycine. 1. A polymorphic transition into a new δ-form. Z. Kristallogr. **220** (2005) 50–57.
[21] Kolesnik, E. N.: The effects of pressure and temperature on the crystal structure of L-serine, Proceedings of the XLII International Scientific Student Conference, Section "Molecular Design and Ecologically Safe Technologies", 2004, April, p. 5.
[22] Boldyreva, E. V.; Kolesnik, E. N.; Drebushchak, T. N.; Ahsbahs, H.: Comparison of the pressure and temperature effects on the amino acid L-serine crystal structure, Proceed. III Intern. Confer. High-Pressure Physics (Chernogolovka, 1-3 June 2004), P-15 www.issp.ac.ru/docs/Cont-Oper2.doc.
[23] Sheldrick, G. M.: Phase-annealing in SHELX-90 – direct methods for larger structures. Acta Cryst. **A46** (1990) 467–473.
[24] Sheldrick, G. M.: Program for crystal structure solution. University of Göttingen, Germany (1997).
[25] Sheldrick, G. M.: Program for refinement of crystal structures. University of Göttingen, Germany. (1997).
[26] Merrill, L.; Bassett, W. A.: Miniature diamond anvil pressure cell for single-crystal X-ray diffraction studies. Rev. Sci. Instrum. **45** (1974) 290–294.
[27] Mao, K. H.; Bell, P. M.: Design and operation of a diamond-window high-pressure cell for the study of single crystal samples loaded cryogenically. Carnegie Inst. Yearbook **79** (1980) 409–411.
[28] Ahsbahs, H.: 20 Jahre Merrill-Bassett Zelle. Z. Kristallogr. Suppl. **9** (1995) 42.
[29] Ahsbahs, H.: Einige experimentelle Aspekte bei der Röntgenbeugung an Einkristallen bei hohem Druck. Z. Kristallogr. Suppl. **11** (1996) 30.
[30] Piermarini, G. J.; Block S.; Barnett, J. D.: Hydrostatic limits in liquids and solids to 100 kbar. J. Appl. Phys. **44** (1973) 5377–5382.
[31] Forman, R. A.; Piermarini, G. J.; Barnett, J. D.; Block, S.: Pressure measurement by utilization of ruby sharp-line luminescence. Science **176** (1972) 284–285.
[32] Piermarini, G. J.; Block, S.; Barnett, J. D.; Forman, R. A.: Calibration of the pressure dependence of the R_1 ruby fluorescence line to 195 kbar. J. Appl. Phys. **46** (1975) 2774–2780.
[33] Hammersley, A.: Fit2D, Version V11.012, hammersley@esrf.fr
[34] Tsybulya, S. V.; Cherepanova, S. V.; Solovyeva, L. P.: Program collection POLYCRYSTAL for IBM/PC. Russ. J. Struct. Chem. (Russian version) **37/2** (1996) 379–382.
[35] Benedetti, E.; Pedone, C.; Sirigu, A.: The crystal structure of L-(-)-serine. Gazzetta Chim. Italiana **103** (1973) 555–561.
[36] Kistenmacher, T. J.; Rand, G. A.; Marsh, R. E.: Refinements of the crystal structures of DL-serine and anhydrous L-serine. Acta Cryst. **B30** (1974) 2573–2578.

[37] Kraus, W.; Nolze, G.: PowderCell for Windows, Vers. 2.3, http://www.bam.de/a_v/v_1/powder/e_cell.html.
[38] Spek, A. L.: PLATON for Windows, 2000, University of Utrecht, The Netherlands.
[39] Nye, J. F.: Physical properties of solids. Oxford University Press, 1957.
[40] Forss, S.: A Raman spectroscopic temperature study of NH_3^+ torsional motion as related to hydrogen bonding in the L-alanine crystal. J. Raman Spectroscopy **12** (1982) 266–273.
[41] Simpson, H. J.; Marsh, R. E.: The crystal structure of L-alanine. Acta Cryst. **20** (1966) 550–555.
[42] Marsh, R. E.: A refinement of the crystal structure of glycine. Acta Cryst. **11** (1958) 654–663.
[43] Iitaka, Y.: The crystal structure of β-glycine. Acta Cryst. **13** (1960) 35–44.
[44] Iitaka, Y.: The crystal structure of γ-glycine. Acta Cryst. **11** (1958) 225–226.
[45] Boldyreva, E. V.; Kivikoski, J.; Howard, J. A. K.: Distortion of crystal structures of some Co^{III} ammine complexes. I. Distortion of crystal structure of $[Co(NH_3)_5NO_2]Cl(NO_3)$ on cooling. Acta Cryst. **B53** (1997) 394–404.
[46] Boldyreva, E. V.; Kivikoski, J.; Howard, J. A. K.: Distortion of crystal structures of some Co^{III} ammine complexes. II. Distortion of crystal structure of $[Co(NH_3)_5NO_2]Cl_2$ and $[Co(NH_3)_5NO_2]Br_2$ on cooling. Acta Cryst. **B53** (1997) 405–414.
[47] Boldyreva, E. V.; Ahsbahs, H.; Naumov, D. Yu.: Distortion of crystal structures of some Co(III) ammine complexes. III. Distortion of crystal structure of $[Co(NH_3)_5NO_2]Cl_2$ at hydrostatic pressures up to 3.5 GPa. Acta Cryst. **B54** (1998) 798–808.
[48] Boldyreva, E. V.; Shakhtshneider, T. P.; Vasilchenko, M. A.; Ahsbahs, H.; Uchtmann, H.: Anisotropic crystal structure distortion of the monoclinic polymorph of acetaminophen at high hydrostatic pressure. Acta Cryst. **B56** (2000) 299–309.
[49] Boldyreva, E. V.; Shakhtshneider, T. P.; Ahsbahs, H.; Sowa, H.; Uchtmann, H.: Effect of high pressure on the polymorphs of paracetamol. J. Therm. Anal. Cal. **68** (2002) 437–452.
[50] Boldyreva, E. V.; Shakhtshneider, T. P.; Ahsbahs, H.; Uchtmann, H.; Burgina, E. B.; Baltakhinov, V. P.: The role of hydrogen bonds in the pressure-induced structural distortion of 4-hydroxyacetanilide crystals. Polish J. Chem. **76** (2002) 1333–1346.
[51] Drebushchak, T. N.; Boldyreva, E. V.: Variable temperature (100–360 K) single-crystal X-ray diffraction study of the orthorhombic polymorph of paracetamol (p-hydroxyacetanilide). Z. Kristallogr. **219** (2004) 506–512.
[52] Boldyreva, E. V.; Shakhtshneider, T. P.; Ahsbahs, H.; Sowa, H.; Uchtmann, H.: Effect of pressure on the crystals of sodium oxalate: anisotropic structural distortion and a polymorphic transition. Russ. J. Struct. Chemi. **43** (2002) 107–113.
[53] Katrusiak, A.: High-pressure X-ray diffraction study on the structure and phase transition of 1,3-cyclohexanedione crystals. Acta Crystallogr. **B46** (1990) 246–256.
[54] Katrusiak, A.: Structure and phase transition of 1,3-cyclohexanedione crystals as a function of temperature. Acta Crystallogr. **B47** (1991) 398–404.
[55] Katrusiak, A.: High-pressure X-ray diffraction study of pentaerithriol. Acta Crystallogr. **B51** (1995) 873–879.